ISBN: 978-3-95450-225-7 ISSN: 2673-5571 doi:10.18429/JACoW-HB2021-MOP03

LONGITUDINAL EMITTANCE MEASUREMENT AT PIP2IT*

Mathias El Baz†, Université Paris Saclay, Orsay, France
Jean-Paul Carneiro, Fermilab, Batavia, USA

Abstract

The PIP-II particle accelerator is a new upgrade to the Fermilab accelerator complex, featuring an 800 MeV H^- superconducting linear accelerator that will inject the beam into the present Fermilab Booster. A test accelerator known as PIP-II Injector Test (PIP2IT) has been built to validate the concept of the front-end of PIP-II [1]. One of the paramount challenges of PIP2IT was to demonstrate a low longitudinal emittance at the end of the front end. Having a low longitudinal emittance is crucial in order to ensure the stability of the beam in the accelerator. We present a longitudinal emittance measurement performed at 14.3 MeV by scanning the SSR1-8 cavity phase and measuring the corresponding beam rms bunch length with a Fast Faraday Cup (FFC) located in the High Energy Transport line (HEBT). The FFC signal is recorded by a high-bandwidth oscilloscope.

INTRODUCTION

The PIP-II Injector Test facility (PIP2IT) is a model of the Front End of PIP-II which will accelerate the H^- ion beam up to 25 MeV. As shown in Fig. 1, the injector is made of an Ion Source, a Low Energy Beam Transport (LEBT) made of three solenoids that matches the beam into a 162.5 MHz Radiofrequency Quadrupole (RFQ), a Medium Energy Beam Transport (MEBT) that prepares the beam for injection into two superconducting (SC) cryomodules: one containing eight Half-Wave Resonators (HWR) cavities operating at 162.5 MHz and one containing eight Single-Spoke Resonator (SSR1) cavities operating at 325 MHz. At the end of the injector a High-Energy Beam Transport (HEBT) brings the beam to a dump.

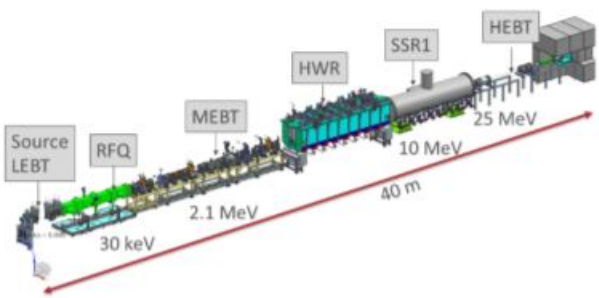

Figure 1: Sketch of PIP2IT.

During normal operation of the injector, the ion source operates with long pulses (usually few ms) and at 20 Hz repetition rate. A beam chopper, located upstream of the third LEBT solenoid, cut pulses of up to 0.55 ms of beam at a repetition rate of 20 Hz. At the exit of the RFQ, the beam has an energy of 2.1 MeV. The MEBT has two purposes: first the MEBT performs a bunch-by-bunch selection using two kickers that decreases the average current in the macro-pulse from 5 mA down to 2 mA, and second the MEBT matches the beam into the HWR cryomodule using 3 buncher cavity (operating at 162.5 MHz), 2 doublets and 7 triplets. During normal operation, the beam is expected to reach an energy of 10.3 MeV at the exit of the HWR cryomodule and 25 MeV at the exit of the SSR1 cryomodule. The transverse focusing is performed by 8 SC solenoids in the HWR cryomodule and by 4 SC solenoid in the SSR1 cryomodule. The HEBT is made of 2 quads.

The goal of the longitudinal emittance measurement performed at PIP2IT is to quantify the beam quality at the end of the injector. A low longitudinal emittance ensures a small bunch length and little variations of the longitudinal momentum inside the bunch, and therefore, a high stability of the beam with negligible losses along the PIP2 linac.

MEASUREMENT SCHEME

Injector Settings

During the commissioning of the PIP2IT injector (from Spring 2020 to Spring 2021), the 3 first HWR cavities were not operational because of a frequency offset for the two first cavities and a coupler issue for the third one. Furthermore, due to multipacting effects, the 2 last HWR cavities (HWR#7 and #8) were operated at lower accelerating gradient than originally anticipated (respectively 8.5 MV/m and 8 MV/m vs 9.7 MV/m). As a consequence of these HWR cavities adjustments, the beam was longitudinally matched from the MEBT into the fourth HWR cavity reaching a beam energy of 8 MeV at the end of the HWR cryomodule and further accelerated to 16.2 MeV by the SSR1 cryomodule. During our longitudinal emittance measurement, and in order to lower the beam power in the Fast Faraday Cup (FFC), the pulse length was limited to 10 µs and the repetition rate to 1 Hz. The average beam current of 5 mA at the exit of the RFQ was chopped down to 2 mA by the 2 MEBT kickers. Under these conditions, the beam was transported with minimal uncontrolled losses until the dump at the end of the HEBT.

Beam Dynamic Simulations

Figure 2 shows the transverse and longitudinal envelope along the PIP2IT injector from Tracewin [2] for the above-mentioned injector settings used during the longitudinal emittance measurement. The simulation starts with a 792×10^3 input distribution at the MEBT ($z = 0$ in Fig. 2). This input distribution was built from a start-to-end model of the Ion Source, LEBT and RFQ, this later being simulated using

* This work was supported by the U.S. Department of Energy under contract No. DE-AC02-07CH11359
† mathias.el-baz@universite-paris-saclay.fr

ISBN: 978-3-95450-225-7 ISSN: 2673-5571 doi:10.18429/JACoW-HB2021-MOP03

the code Toutatis [2]. The injector was modeled in Tracewin using 3*D* fields for all cavities, solenoids, quadrupoles and correctors.

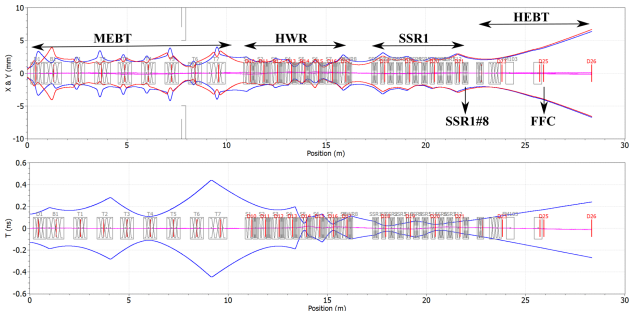

Figure 2: Transverse (upper) and Longitudinal (lower) envelope along the PIP2IT injector for the phase scan measurement. The beam is longitudinally matched from the MEBT into the 4th HWR cavity. From Tracewin.

Description of the Cavity Phase Scan

The schematic of the cavity phase scan measurement section is represented in Fig. 3. The objective is to estimate the longitudinal emittance at the entrance of the eighth and last SSR1 cavity (noted SSR1#8 on Fig. 3). The SSR1#8 cavity phase is scanned from −10° to −45° (with a 5° step) and at fixed field amplitude of 10 MV/m changing the beam energy from 16.2 MeV to about 15.6 MeV according to Tracewin.

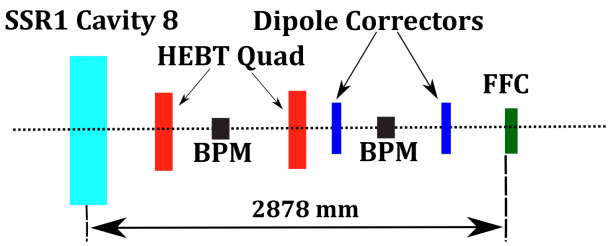

Figure 3: Schematic of the section of interest for the scan.

The cavity acts like a thin lens whose focal length depends on its phase. Therefore, the bunch length at an upstream location varies during the scan. We can reconstruct the longitudinal emittance from the variation of the bunch length. The ions are collected at the end the HEBT by a FFC and the corresponding waveforms are recorded by a high-bandwidth oscilloscope located outside the cave enclosure and with a 10 ps interpolation sampling. The rms bunch length at the FFC is estimated using a Gaussian fit of the FFC waveform. The FFC has a collimating aperture of 0.8 mm and efforts have been made during the cavity phase scan to keep the beam centered with the FFC aperture using BPMs and correctors located upstream of the FFC. Two quadrupoles located between the cavity and the FFC have also been used during the measurement in order to maximize the signal at the FFC. As indicate in Fig. 3, the distance between the middle of the SSR1#8 cavity and the FFC is 2878 mm. A detailed description of the FFC is given in [3] and [4].

Analysis of the Waveform

Figure 4 shows a FFC signal for operation of the SSR1#8 cavity at 10 MV/m and a phase of −15°. The signal is fitted with a Gaussian curve and the rms bunch length of the beamlet is extracted. A detailed analysis of the beam distribution at the FFC obtained from Tracewin simulation have shown that the rms bunch length of the beamlet is representative of the rms bunch length of the core of the beam representing about 90% of the full beam.

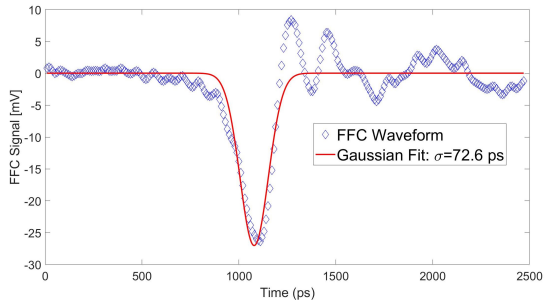

Figure 4: FFC waveform for a field on SSR1#8 of 10 MV/m and a phase of −15° with Gaussian fit, 10 µs pulse, 1 Hz, 2 mA average beam current.

As discussed, the FFC waveform analysis is based on the assumption of a Gaussian-shape bunch. However, as shown in Fig. 4, the bunch diverges from the Gaussian model. The bunch is skewed to the right and the baseline oscillates after the bunch. These distortions are very unlikely due to discrepancies of the beam. Since the oscilloscope is out of the cave, the long cable between the FFC and the oscilloscope could explain the skewed feature characteristic of cable dispersion. The oscillations after the bunch are likely due to reflections near the FFC. We estimate the error between the Gaussian bunch length RMS and the real bunch length to be below 7%. The estimation of the longitudinal emittance with error bar (and discussed in the last section) is deduced from the uncertainty on the bunch length.

LONGITUDINAL EMITTANCE RECONSTRUCTION

The beam is first focused by the SSR1-8 cavity and needs to pass a 2878 mm drift before being collected by the FFC. The transport matrix M modelling the evolution of the beam between the input of SSR1-8 and the FFC is the product of the drift matrix and the SSR1-8 matrix [5]:

$$M(\Phi_s) = \underbrace{\begin{pmatrix} 1 & \frac{L}{\gamma_f^2} \\ 0 & 1 \end{pmatrix}}_{\text{Drift}} \times \underbrace{\begin{pmatrix} 1 & 0 \\ \frac{-2\gamma^2 k sin(\Phi_s)}{(\beta\gamma)_f} & \frac{(\beta\gamma)_i}{(\beta\gamma)_f} \end{pmatrix}}_{RF}$$

with:

$$k \hat{=} -\frac{\pi}{\beta^2\gamma^2\lambda}\frac{Q}{A}\frac{E_0 T L}{m_u c^2}$$

where $(\beta\gamma)_i$ and $(\beta\gamma)_f$ are respectively the relativistic coefficients at the entrance and the exit of SSR1-8, L is the drift

ISBN: 978-3-95450-225-7 ISSN: 2673-5571 doi:10.18429/JACoW-HB2021-MOP03

length, Φ_s is the cavity phase, and k is the focusing strength of the cavity. The phase dependence of M is also contained in $(\beta\gamma)_f$. M is numerically calculated for each cavity phase using the different values of $(\beta\gamma)_f$ given by the Tracewin simulation.

The beam matrix at the FFC is linked to the beam matrix at the input of SSR1-8 by:

$$\Sigma_{FFC}(\phi_s) = M(\phi_s)\,\Sigma_{SSR1-8} M(\phi_s)^T$$

One can notice that the determinant of the beam matrix is not conserved since the determinant of M is strictly less than 1. Therefore, the longitudinal emittance and the beam energy at the output of SSR1-8 are phase dependent. Only the (1,1) coordinate of Σ_{FFC} is measured and can be expressed as a function of the M and Σ_{SSR1-8} coordinates:

$$\begin{aligned}\sigma_z^{FFC}(\phi_s)^2 &= \Sigma_{11}^{SSR1} M_{11}(\phi_s)^2 + 2M_{11}(\phi_s) M_{12}(\phi_s) \Sigma_{12}^{SSR1} \\ &\quad + M_{12}^2(\phi_s) \Sigma_{22}^{SSR1} \\ &= \underbrace{\Sigma_{11}^{SSR}}_{a} X^2 + \underbrace{2\Sigma_{12}^{SSR}}_{b} XY + \underbrace{\Sigma_{22}^{SSR}}_{c} Y^2\end{aligned}$$

where $X = M_{11}(\phi_s)$ and $Y = M_{12}(\phi_s)$. $\sigma_z^{FFC}(\phi_s)^2$ is a polynomial function of X and Y. We can fit the evolution of $\sigma_z^{FFC}(\phi_s)^2$ in order to estimate the polynomial coefficients a,b and c (Fig. 5). The longitudinal emittance measurement is computed from the estimation of these coefficients:

$$\begin{aligned}\epsilon_z^{SSR1} &= (\beta\gamma)_i \sqrt{ac - \frac{1}{4}b^2} \\ &= (\beta\gamma)_i \sqrt{\Sigma_{11}^{SSR1}\Sigma_{22}^{SSR1} - \left(\Sigma_{12}^{SSR1}\right)^2} \\ &= 0.29\,\text{mm}\cdot\text{mrad}\end{aligned}$$

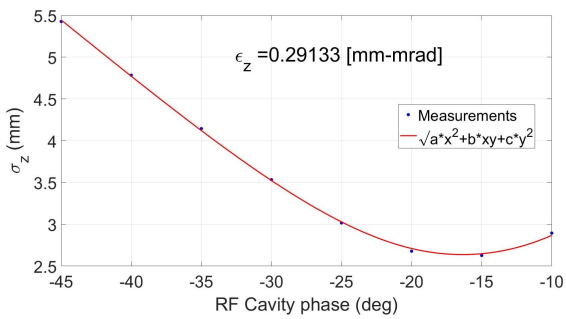

Figure 5: Measured rms bunch length at the FFC as a function of the SSR1#8 cavity phase and reconstruction of the longitudinal emittance at SSR1#8 cavity entrance.

DISCUSSION

As previously mentioned, we estimate the error between the Gaussian bunch length RMS and the real bunch length to be below 7%. The estimation of the longitudinal emittance with error bar is deduced from the uncertainty on the bunch length and estimated to be:

$$\epsilon_z^{SSR1} = (0.29 \pm 0.02)\text{mm.mrad}.$$

This measured emittance is in good agreement with the Tracewin simulation reported in Fig. 6 which shows the 90% longitudinal phase space at the SSR1#8 cavity and the corresponding longitudinal emittance of 0.3 mm·mrad.

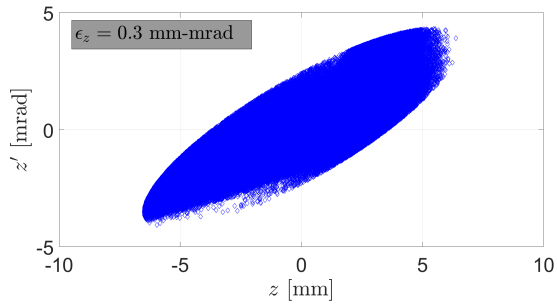

Figure 6: Simulated 90% longitudinal phase space distribution at the entrance of the SSR1#8 cavity. From Tracewin.

The longitudinal phase space distribution of Fig. 6 corresponds to the distribution at the entrance of the SSR1#8 cavity for the envelope shown in Fig. 2 and for which 10% of the beam with the largest longitudinal action has been removed. Analysis of the Tracewin distribution at the FFC shows that the core of the beam sampled by the FFC of about 0.8 mm diameter is representative of the rms bunch length of about 90% of the full beam. As a consequence, we consider the emittance measurement reported in this document as being representative of the core (about 90%) of the beam and in good agreement with simulations.

ACKNOWLEDGEMENT

We want to thank the team members for their expertise and assistance on all the aspects of our study and for their help in writing this article. We especially thank Eduard Pozdeyev, Alexander Shemyakin, Arun Saini, Bruce Hanna and Lionel Prost for their help in the analysis and Victor Scarpine for giving us his expertise in instrumentation.

REFERENCES

[1] PIP-II Collaboration, "PIP-II Reference Design Report", FNAL, Batavia, IL, USA, 2015.

[2] Tracewin and Toutatis codes, http://irfu.cea.fr/Sacm/logiciels/

[3] A. Shemyakin *et al.*, "Characterization of the beam from the RFQ of the PIP-II Injector Test" , in *Proc. IPAC'17*, Copenhagen, Denmark, May 2017, pp. 2425–2428. doi:10.18429/JACoW-IPAC2017-TUPVA139

[4] J.-P. Carneiro *et al.*, "Longitudinal beam dynamics studies at the PIP-II injector test facility", *International Journal of Modern Physics A*, Vol. 34, no. 36, p. 1942013, 2019. doi:10.1142/S0217751X19420132

[5] USPAS Notes, Chapter 3: Basic of beam dynamics, 2013. https://uspas.fnal.gov/materials/13Duke/SCL_Chap3.pdf